International Journal For Advanced Research In Science & Technology
A peer reviewed international journal
www.ijarst.in
ISSN: 2457-0362

Simulation of Three-Port Converterwith Grid Connectedsystem for Hybrid Power Distributed and Generation System

1.Dr. M. Rama Prasad Reddy,2 P Puneeth Kumar ,3 M Mudassir Rehman,4 K Veeresh Kumar,5 N Venkatesh,6 B Vamsi Sai
1Professor, 2,3,4,5,6 B Tech Scholars
1,2,3,4,5.6Department of electrical and electronics engineering,
1,2,3,4,5.6G. Pullaiah College of Engineering and Technology (Autonomous),Nandikotkur Rd,
Near Venkayapalle, Pasupala Village Kurnool AndhraPradesh 518002

Abstract:Conventional methodology for electrical power generation is vulnerable due to environmental limitations and the availability of fuel. Distributed generation, offering virtuous benefits to the market partakers, is trending in electrical power system in modern era. Hybrid distributed power generating units combining battery storage and renewable sources have attracted in recent days pushing back the conventional systems. Conventional systems use two separate converters for PV and battery source. This paper proposes an energy management and control strategy for the PV/battery hybrid distributed power generation systems with only one integrated three-port power converter. Energy management and control strategy are proposed to realize the power balance among three ports in different operating scenarios, which comprehensively takes both the maximum power point tracking (MPPT) and the battery charging/discharging management into consideration. The simulation model and the results are analyzed using MATLAB/Simulink.

KEYWORDS: Distributed generation, maximum power point tracking (MPPT), PV/battery hybrid distributed power generation systems

(I) Introduction

Rapid depletion of fossil fuels and global warming has necessitated an urgent need for alternative sources of energy to cater thecontinuously increasing energy demand. The environmental effects and the cost of central power plants are causing a large focus onrenewable energies. The power plants are using fossil fuels which result in greenhouse gas emissions. These greenhouse gasemissions have a significant effect on the planet especially with the growth of the population and the corresponding increase ofenergy consumption. Due to the limitation of conventional resources of fossil fuels, it has compelled the evolution of hybrid powersystem. Therefore, new ways to balance the load demand is by integrating RES into the system.Hybrid system enables the incorporation of renewable energy sources and transferable the dependency on fossil fuels, whilesustaining the balance between supply and demand. The significant characteristic of hybrid power system includes, systemreliability, operational efficiency [1]. The hybrid power system enables to overcome the limitations in wind and photovoltaicresources since their performance characteristics depends upon the unfavorable changes in environmental conditions. It is probableto endorse that hybrid stand-alone electricity generation systems are usually more reliable and less costly than systems that dependon a single source of energy [2]. On other hand one environmental condition can make one type of RES more profitable than other.

For example, Photovoltaic (PV) system is ideal for locations having more solar illumination levels and Wind power system is idealfor locations having better wind flow conditions [3].Thus a PV system consisting of PV array, Maximum Power Point Tracking (MPPT) boost converters, and Wind power systemconsisting of wind turbine, PMSG, rectifier and MPPT boost converter is integrated into Solar-Wind hybrid power system(SWHPS). The efficiency and reliability of the SWHPS mainly depends upon the control strategy of the MPPT boost converter.The solar and wind power generation cannot operate at Maximum power point (MPP) without proper control logic in the MPPTboost converter. If the MPP is not tracked by the controller the power losses will occur

International Journal For Advanced Research In Science & Technology
A peer reviewed international journal
www.ijarst.in
ISSN: 2457-0362

in the system and in spite of wind and solarpower availability, the output voltage of the hybrid system will not boost up to the required value [4]. The output voltage of the PVand Wind power generation are quite low as compared with the desired operating level. So, this output voltage is brought to desiredoperating value of 220V using Boost converter with MPPT controller at each source.Hybrid PV–wind-based generation of electricity and its interface with the power grid are the important research areas. Chen etal. [5], [6] have proposed a multi-input hybrid PV–wind power generation system which has a buck/buck– boost-fused multi-inputdc–dc converter and a full-bridge dc–ac inverter. This system is mainly focused on improving the dc-link voltage regulation. In thesix-arm converter topology proposed in [7], the outputs of a PV array and wind generators are fed to a boost converter to match thedc-bus voltage. The steady-state performance of a grid-connected hybrid PV and wind system with battery storage is analyzed in[8]. This paper focuses on system engineering, such as energy production, system reliability, unit sizing, and cost analysis. In [9], ahybrid PV–wind system along with a battery is presented, in which both sources are connected to a common dc-bus throughindividual power converters. In addition, the dc-bus is connected to the utility grid through an inverter.The use of multi-input converter for hybrid power systems is attracting increasing attention because of reduced componentcount, enhanced power density, compactness, and centralized control. Due to these advantages, many topologies are pro-posed, andthey can be classified into three groups, namely, non-isolated, fully isolated, and partially isolated multiport topologies.

All the power ports in non-isolated multiport topologies share a common ground. To derive the multiport dc–dc converters, aseries or parallel configuration is employed in the input side [10]–[14]. Some components can be shared by each input port.

However, a time-sharing control scheme couples each input port, and the flexibility of the energy delivery is limited. The series orparallel configuration can be extended at the output to derive multiport dc–dc converters [15]. However, the power componentscannot be shared. All the topologies in non-isolated multiport are mostly combinations of the basic topology units, such as the buck,the boost, the buck–boost, or the bidirectional buck/boost topology unit. These time-sharing-based multiport topologies promiselow cost and easy implementation. However, a common limitation is that power from multiple inputs cannot be simultaneously transferred to the load. Furthermore, matching wide voltage ranges will be difficult in these circuits. This made the researchers toprefer isolated multiport converters compared with non-isolated multiport dc–dc converters.

The proposed system has two renewable power sources, load, grid, and battery. Hence, a power flow management system isessential to balance the power flow among all these sources. The main objectives of this system are as follows.

1) To explore a multi-objective control scheme for optimal charging of the battery using multiple sources.

2) Supplying uninterruptible power to loads.

3) Ensuring the evacuation of surplus power from the renewable sources to the grid, and charging the battery from the grid asand when required.

2 Basic Analysis

The proposed PV/battery hybrid distributed power generatio system is shown in Fig. 1. This is a three-port system interfacing a PV, an ESS unit (a battery for example) and a DC load. The battery serves as an energy buffer, which means it can be charged or discharged to balance the power flow in the PV/battery hybrid power system. As shown in Fig. 1, the phase-shift full-bridge DC-DC converter interfacing the PV and the load shares power switches with the integrated bidirectional buck/boost converter interfacing the battery, based on which the power density of the system is enhanced compared with the conventional topology consisting of the independent phase-shift full-bridge DC-DC converter and bidirectional converter.

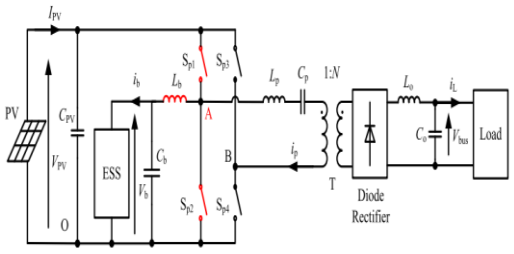

Fig1. The proposed PV/battery hybrid distributed power generation system.

International Journal For Advanced Research In Science & Technology
A peer reviewed international journal
www.ijarst.in
ISSN: 2457-0362

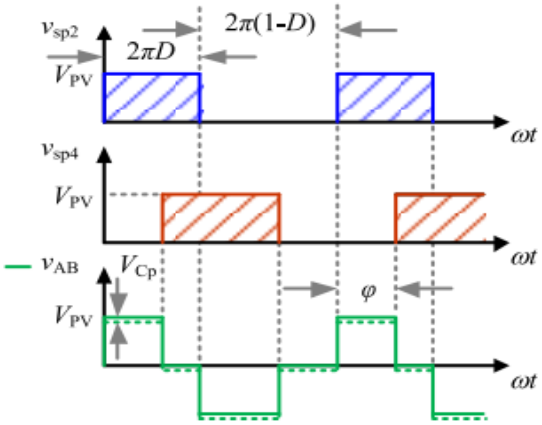

FIGURE 2. Modulation strategy of the full bridge with the phase shift angle' and the duty cycle D.

A modified phase-shift modulation scheme is adopted for the primary full bridge as shown in Fig. 2. Two switching legs of the primary full bridge are phase shifted by the angle '. In addition, the duty cycle of switches Sp1 and Sp2 on leg A can be regulated, while the duty cycle of the other two switches is fixed at 50%.

The integrated bidirectional buck/boost converter interfacing the battery at the primary side of the HF transformer is highlighted in Fig. 2. The battery, capacitor Cb, inductor Lb, two power switches of the leg A and the PV side bus form a bidirectional buck/boost topology inherently. When the battery is charged with ib> 0, the topology operates in the buck mode. When the battery is discharged with ib< 0, then the topology operates in the boost mode. Therefore, the bidirectional power flow can be achieved for the battery with the charging/discharging management requirement.

According to the buck/boost operating principle, since the battery voltage Vb can be considered as almost constant during the normal SOC period, the PV output voltage VPV can be regulated to achieve MPPT by control of the duty cycle D. Assuming that the inductor Lb is large enough, VPV is derived as

$$V_{PV} = V_b/D \tag{1}$$

Where D represents the duty cycle of the switch Sp1 of leg A as shown in Fig. In addition, the phase shift angle ' is adopted as another control variable to obtain the required DC bus voltage Vbus. Due to the asymmetric modulation with two legs of the full bridge, vAB contains a DC component, which can compromise the normal operation of the HF transformer.

In this paper, a DC blocking capacitor Cp is incorporated to prevent the HF transformer from saturation. According to the volt-second balance principle for the inductor Lp and the HF transformer, the DC blocking capacitor Cp voltage VCp is derived as

$$V_{Cp} = V_{PV}\left(D - \frac{1}{2}\right) \tag{2}$$

Based on the volt-second balance principle for the inductor Lo and assuming Lo is large enough, the DC bus voltage Vbus can be expressed as

$$V_{bus} = N\left\{\frac{\varphi}{2\pi}(V_{PV}-V_{Cp})+\left(\frac{1}{2}+\frac{\varphi}{2\pi}-D\right)(V_{PV}+V_{Cp}) + \left[1-\left(\frac{1}{2}+\frac{\varphi}{2\pi}-D+\frac{\varphi}{2\pi}\right)\right]|V_{Cp}|\right\} \tag{3}$$

Where the turns ratio of the transformer is defined as 1:N. Then the DC bus voltage Vbus can be derived as

$$V_{bus} = \begin{cases} NV_{PV}\dfrac{\varphi}{\pi}\left(\dfrac{3}{2}-D\right), & D > \dfrac{1}{2} \\ NV_{PV}\left[\dfrac{\varphi}{\pi}\left(\dfrac{1}{2}+D\right)+\dfrac{1}{2}-2D^2\right], & D < \dfrac{1}{2}. \end{cases} \tag{4}$$

According to Fig. 3, the following constraints need to be applied for the modulation scheme as

$$\begin{cases} D > \dfrac{\varphi}{2\pi} \\ \dfrac{1}{2}+\dfrac{\varphi}{2\pi}-D > 0 \end{cases} \tag{5}$$

International Journal For Advanced Research In Science & Technology
A peer reviewed international journal
www.ijarst.in
ISSN: 2457-0362

Which can be further derived as' and D serve as the only two control variables for the proposed PV/battery hybrid distributed power generation system, based on which a corresponding energy management and control strategy is proposed in the following section.

$$\frac{\varphi}{2\pi} < D < \frac{\varphi}{2\pi} + \frac{1}{2} \tag{6}$$

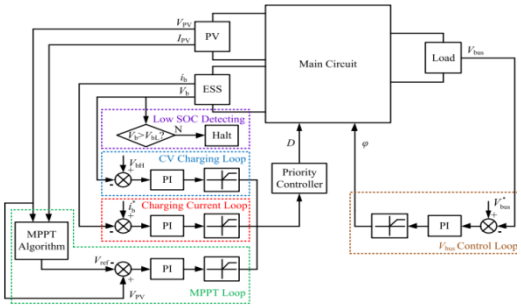

FIGURE 3. Control algorithm of the proposed PV/battery hybrid distributed power generation system.

3. CONTROL ALGORITHM

The control algorithm of the proposed PV/battery hybrid distributed power generation system is shown in Fig. 3. Various MPPT techniques have been introduced in [19]. In this paper, only the conventional incremental conductance MPPT technique is adopted since the improvement of the MPPT algorism is not the focus of this paper. As shown in Fig. 3, the phase shift angle'of the full bridge is used to control the load side DC bus voltage *V*bus through a PI controller. The PV reference voltage *V*ref is obtained by the basic incremental conductance MPPT algorithm. In addition, a low SOC detecting part is incorporated in the control system to temporarily halt the operation of the system (such as setting the phase shift angle'as zero) when the battery voltage *V*b drops to a low value *V*bL. The duty cycle *D* serves as the key control variable to achieve the power balance and automatic control in different operation scenarios of the whole power generation system. There are three control loops competing to take charge of the duty cycle *D*, namely the constant voltage (CV) charging loop, charging current loop and MPPT loop. The priority controller determines which control loop to enable. The overall objective is to achieve the power balance of the whole power system and automatic battery charging/discharging management, while have the PV to operate at the maximum power point if possible. In this paper, the priority controller is to obtain the minimum value among three control loop outputs. For example, when the load power PL is larger than the PV maximum output power PMPP but within the most power that the PV and battery can supply in combination, the battery would operate in the discharging mode, and therefore the battery charging current ib would turn negative, which results in the saturation for the output of the charging current loop.

Then in this case the MPPT control loop would be enabled (assuming the battery voltage Vb is lower than the CV charging voltage VbH and the CV charging loop is disabled), and the duty cycle D would be regulated until the PV operates near the maximum power point. It is noted that the battery serves as a power balance port in this case.

When the load power is relatively small, there can be much surplus power from the PV supposing the MPPT control loop is enabled, which can cause high battery charging power beyond the specific battery charging requirements. In this case the input error signal of the charging current control loop would turn negative, which means the corresponding loop would take charge over the duty cycle D (assuming the battery voltage Vb is lower than the CV charging voltage VbH and the CV charging loop is disabled). Therefore the battery would operate in the constant current (CC) charging mode at a preset level of i∗ b. It is noted that the PV serves as a power balance port in this case and the operating point of the PV would be regulated accordingly to achieve the power balance of the system.

For the CV charging loop, when the battery voltage Vb reaches the preset CV charging voltage VbH, the CV charging loop is enabled and the battery would operate in the CV charging mode. Since the charging power is unstable and uncontrollable for the CV charging mode, the operating point of the PV would change through the CV charging process to achieve the power balance. Potential operation scenarios of

International Journal For Advanced Research In Science & Technology
A peer reviewed international journal
www.ijarst.in
ISSN: 2457-0362

the proposed PV/battery hybrid distributed power generation system under various power conditions among three ports are illustrated below as scenario 1 to scenario 7.

1) Scenario 1: The load power is larger than the most power that the PV and battery can supply in combination. In this case either the whole system needs to be halted, or measures such as the load shedding needs to be taken.

2) Scenario 2: The load power is larger than the PV maximum output power PMPP, but within the most power that the PV and battery can supply in combination. In this case the MPPT control loop would be enabled to utilize the most of the solar energy under the specific irradiance and temperature conditions. In the meantime, the battery would operate in the discharging mode and supply a part of the load power, which achieves the power balance for the system.

3) Scenario 3: The PV maximum power PMPP just equals to the load power. In this case the battery would not be charged or discharged and the PV supplies the load power solely at the maximum power point.

4) Scenario 4: The PV maximum power PMPP is larger than the load power, and the surplus power from the PV is within the maximum charging power of the battery. In this case, the MPPT control loop would be enabled and the PV would supply the load and charge the battery in the meantime. The battery serves as the power balance port of the system in this case.

5) Scenario 5: The PV maximum power PMPP is larger than the total of the load power and the maximum charging power of the battery under the specific irradiance and temperature conditions. In this conditions. In this case the battery charging current ib control loop would be enabled and the MPPT control loop would be disabled. The battery would operate in the constant current charging mode at a preset level of i∗ b. In the meantime, the operating point of the PV would be regulated accordingly until the power balance of the system can be achieved.

6) Scenario 6: The PV output power is near zero (for example in the evening) and the load power is larger than the maximum discharging power of the battery. In this case either the whole system needs to be halted, or measures such as the load shedding needs to be taken.

7) Scenario 7: The PV output power is near zero and the load power is within the maximum discharging power of the battery. In this case the battery would operate in the discharging mode as the only power source.

A brief illustration about different potential operation scenarios mentioned above is shown in Table 1. PMax DCHG represents the maximum discharging power of the battery and PMax CHG represents the maximum charging power of the battery, and both are determined by the specific application requirements of the battery. In addition, a flow diagram of the proposed control algorithm is presented in Fig. 4.

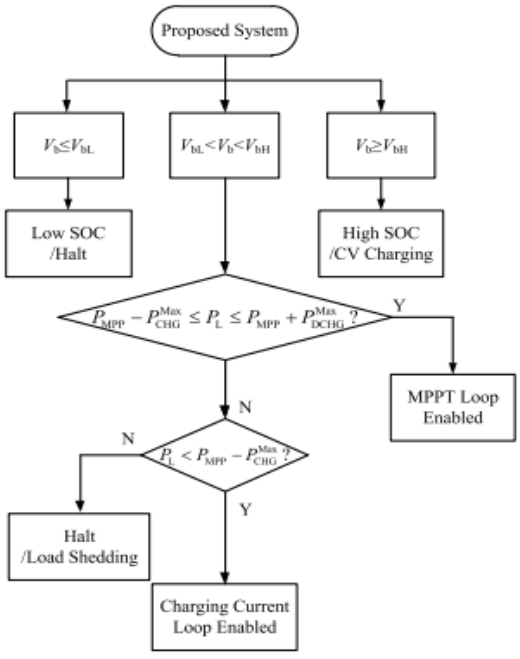

FIGURE 4. Flow diagram of the proposed control algorithm.

International Journal For Advanced Research In Science & Technology
A peer reviewed international journal
www.ijarst.in
ISSN: 2457-0362

TABLE 1. Operation scenarios of the system.

Scenarios	Power Conditions	MPPT
1	$P_L > P_{MPP} + P_{DCHG}^{Max}$	-
2	$P_{MPP} < P_L \leq P_{MPP} + P_{DCHG}^{Max}$	Enabled
3	$P_L = P_{MPP}$	Enabled
4	$P_{MPP} - P_{CHG}^{Max} \leq P_L < P_{MPP}$	Enabled
5	$P_L < P_{MPP} - P_{CHG}^{Max}$	-
6	$P_{PV}=0$, $P_L > P_{DCHG}^{Max}$	-
7	$P_{PV}=0$, $P_L \leq P_{DCHG}^{Max}$	-

4. INDUCTION MOTOR

An asynchronous motor type of an induction motor is an AC electric motor in which the electric current in the rotor needed to produce torque is obtained by electromagnetic induction from the magnetic field of the stator winding. An induction motor can therefore be made without electrical connections to the rotor as are found in universal, DC and synchronous motors. An asynchronous motor's rotor can be either wound type or squirrel-cage type.

Three-phase squirrel-cage asynchronous motors are widely used in industrial drives because they are rugged, reliable and economical. Single-phase induction motors are used extensively for smaller loads, such as household appliances like fans. Although traditionally used in fixed-speed service, induction motors are increasingly being used with variable-frequency drives (VFDs) in variable-speed service. VFDs offer especially important energy savings opportunities for existing and prospective induction motors in variable-torque centrifugal fan, pump and compressor load applications. Squirrel cage induction motors are very widely used in both fixed-speed and variable-frequency drive (VFD) applications. Variable voltage and variable frequency drives are also used in variable-speed service.

In both induction and synchronous motors, the AC power supplied to the motor's stator creates a magnetic field that rotates in time with the AC oscillations. Whereas a synchronous motor's rotor turns at the same rate as the stator field, an induction motor's rotor rotates at a slower speed than the stator field. The induction motor stator's magnetic field is therefore changing or rotating relative to the rotor. This induces an opposing current in the induction motor's rotor, in effect the motor's secondary winding, when the latter is short-circuited or closed through external impedance. The rotating magnetic flux induces currents inthe windings of the rotor; in a manner similar to currents induced in a transformer's secondary winding(s). The currents in the rotor windings in turn create magnetic fields in the rotor that react against the stator field. Due to Lenz's Law, the direction of the magnetic field created will be such as to oppose the change in current through the rotor windings. The cause of induced current in the rotor windings is the rotating stator magnetic field, so to oppose the change in rotor-winding currents the rotor will start to rotate in the direction of the rotating stator magnetic field. The rotor accelerates until the magnitude of induced rotor current and torque balances the applied load. Since rotation at synchronous speed would result in no induced rotor current, an induction motor always operates slower than synchronous speed.The difference, or "slip," between actual and synchronous speed varies from about 0.5 to 5.0% for standard Design B torque curve induction motors. The induction machine's essential character is that it is created solely by induction instead of being separately excited as in synchronous or DC machines or being self-magnetized as in permanent magnet motors.

For rotor currents to be induced the speed of the physical rotor must be lower than that of the stator's rotating magnetic field ($\boldsymbol{n_s}$); otherwise the magnetic field would not be moving relative to the rotor conductors and no currents would be induced. As the speed of the rotor drops below synchronous speed, the rotation rate of the magnetic field in the rotor increases, inducing more current in the windings and creating more torque. The ratio between the rotation rate of the magnetic field induced in the rotor and the rotation rate of the stator's rotating field is called slip. Under load, the speed drops and the slip increases enough to create sufficient torque to turn the load. For this reason, induction motors are sometimes referred to as asynchronous motors. An induction motor can be used as an induction generator, or it can be unrolled to form a linear induction motor which can directly generate linear motion.

Synchronous Speed:

The rotational speed of the rotating magnetic field is called as synchronous speed.

International Journal For Advanced Research In Science & Technology
A peer reviewed international journal
www.ijarst.in
ISSN: 2457-0362

$$Ns = \frac{120 \times f}{P} \quad (RPM) \tag{7}$$

Where, f = frequency of the supply
P = number of poles

Slip:

Rotor tries to catch up the synchronous speed of the stator field, and hence it rotates. But in practice, rotor never succeeds in catching up. If rotor catches up the stator speed, there won't be any relative speed between the stator flux and the rotor, hence no induced rotor current and no torque production to maintain the rotation. However, this won't stop the motor, the rotor will slow down due to lost of torque, and the torque will again be exerted due to relative speed. That is why the rotor rotates at speed which is always less the synchronous speed.
The difference between the synchronous speed (Ns) and actual speed (N) of the rotor is called as slip.

$$\% \text{ slip} \quad s = \frac{Ns - N}{Ns} \times 100 \tag{8}$$

(a) General information regarding micro grid

As electric distribution technology steps into the next century, many trends are becoming noticeable that will change the requirements of energy delivery. These modifications are being driven from both the demand side where higher energy availability and efficiency are desired and from the supply side where the integration of distributed generation and peaks having technologies must be accommodated.

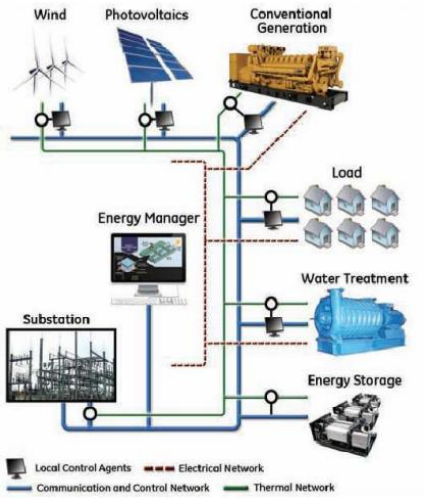

Fig 5. Microgrid power system

Power systems currently undergo considerable change in operating requirements mainly as a result of deregulation and due to an increasing amount of distributed energy resources (DER). In many cases DERs include different technologies that allow generation in small scale (micro sources) and some of them take advantage of renewable energy resources (RES) such as solar, wind or hydro energy. Having micro sources close to the load has the advantage of reducing transmission losses as well as preventing network congestions. Moreover, the possibility of having a power supply interruption of end-customers connected to a low voltage (LV) distribution grid (in Europe 230 V and in the USA 110 V) is diminished since adjacent micro sources, controllable loads and energy storage systems can operate in the islanded mode in case of severe system disturbances. This is identified nowadays as a micro grid. Figure 5 depicts a typical micro grid. The distinctive micro grid has the similar size as a low voltage distribution feeder and will rare exceed a capacity of 1 MVA and a geographic span of 1 km. Generally more than 90% of low voltage domestic customers are supplied by underground cable when the rest is supplied by overhead lines. The micro grid often supplies both electricity and heat to the customers by means of combined heat and power plants (CHP), gas turbines, fuel cells, photovoltaic (PV) systems, wind turbines, etc. The energy storage systems usually include batteries and flywheels. The storing device in the micro grid is equivalent to the rotating reserve of large generators

International Journal For Advanced Research In Science & Technology
A peer reviewed international journal
www.ijarst.in
ISSN: 2457-0362

in the conventional grid which ensures the balance between energy generation and consumption especially during rapid changes in load or generation.

From the customer point of view, micro grids deliver both thermal and electricity requirements and in addition improve local reliability, reduce emissions, improve power excellence by supportive voltage and reducing voltage dips and potentially lower costs of energy supply. From the utility viewpoint, application of distributed energy sources canpotentially reduces the demand for distribution and transmission facilities. Clearly, distributed generation located close to loads will reduce flows in transmission and distribution circuits with two important effects: loss reduction and ability to potentially substitute for network assets. In addition, the presence of generation close to demand could increase service quality seen by end customers. Micro grids can offer network support during the time of stress by relieving congestions and aiding restoration after faults. The development of micro grids can contribute to the reduction of emissions and the mitigation of climate changes. This is due to the availability and developing technologies for distributed generation units are based on renewable sources and micro sources that are characterized by very low emissions.

There are various advantages offered by micro grids to end-consumers, utilities and society, such as: improved energy efficiency, minimized overall energy consumption, reduced greenhouse gases and pollutant emissions, improved service quality and reliability, cost efficient electricity infrastructure replacement.

Technical challenges linked with the operation and controls of micro grids are immense. Ensuring stable operation during network disturbances, maintaining stability and power quality in the islanding mode of operation necessitates the improvement of sophisticated control strategies for micro grid's inverters in order to provide stable frequency and voltage in the presence of arbitrarily varying loads. In light of these, the micro grid concept has stimulated many researchers and attracted the attention of governmental organizations in Europe, USA and Japan. Nevertheless, there are various technical issues associated with the integration and operation of micro grids.

5. SIMULATION RESULTS:

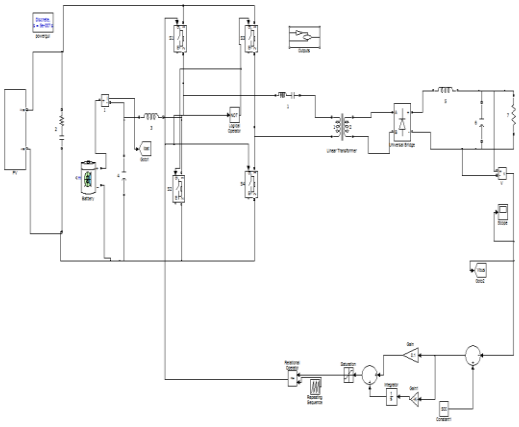

Fig 6 Diagram of Proposed System

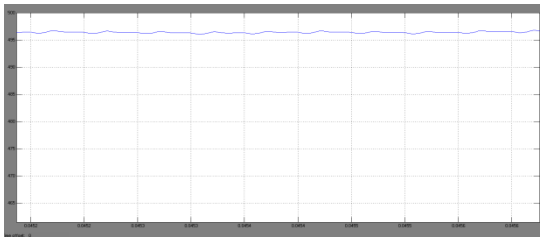

(a) DC bus voltage V bus;

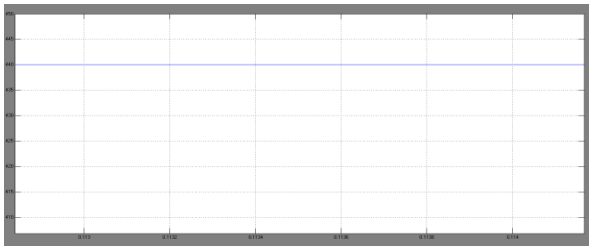

(b) PV voltage VPV;

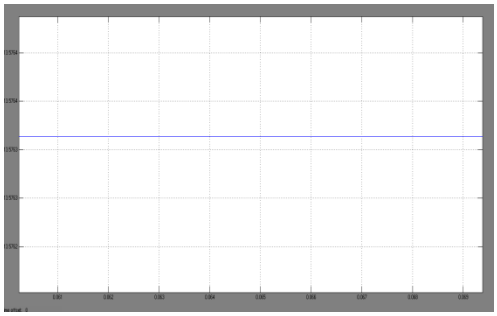

(c) PV current IPV;

International Journal For Advanced Research In Science & Technology
A peer reviewed international journal
www.ijarst.in
ISSN: 2457-0362

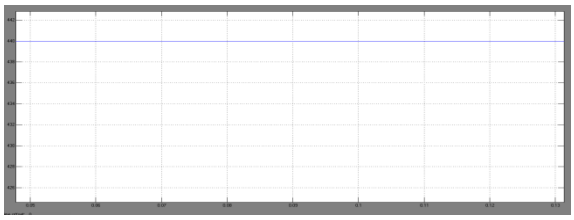

(d) PV reference voltage Vref;

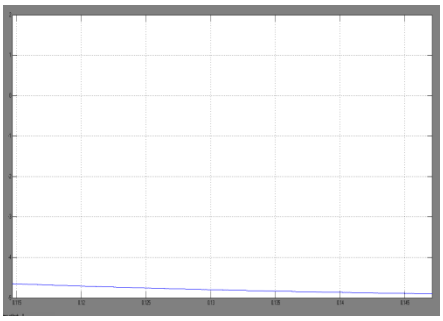

FIGURE 7 Steady state simulation results of operation scenario 2. (a) DC bus voltage Vbus; (b) PV voltage VPV; (c) PV current IPV; (d) PV reference voltage Vref; (e) Batter charging current ib.

The steady state simulation results of the operation are shown in Fig. 7. The simulation conditions are as follows: Irradiance D 1000 W/m2, Temperature D 25 ◦C), the load power PL D 10 kW. By regulating the phase shift angle ' through a PI controller, the DC bus voltage Vbus is controlled at the present value Vbus∗ D 500 V, which is shown in Fig. 7 (a). From Fig. 7 (b), Fig. 7 (c) and Fig. 7 (d), since the MPPT loop is enabled in this scenario, the PV operates at the maximum power point with VPV controlled near the ideal value VMPP D 435 V and IPV controlled near the ideal value IMPP D 22 A. According to Fig. 7 (e), the battery operates in the discharging mode and supplies a part of the load power.

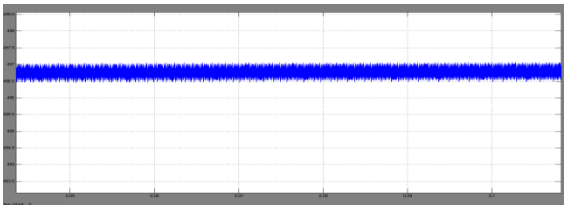

(a) DC bus voltage V bus;

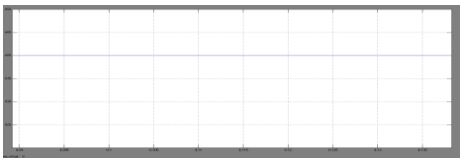

(b) PV voltage VPV;

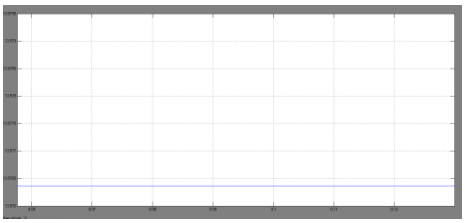

(c) PV current IPV;

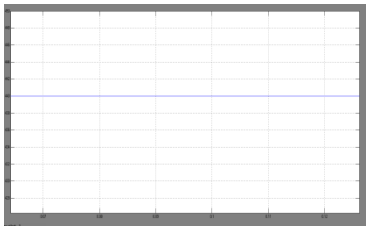

(d) PV reference voltage Vref;

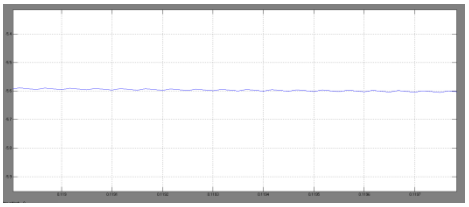

(e) Battery charging current ib.

FIGURE 8. Steady state simulation results of operation scenario 4. (a) DC bus voltage Vbus; (b) PV voltage VPV; (c) PV current IPV; (d) PV reference voltage Vref; (e) Battery charging current ib.

The steady state simulation results of the operation are shown in Fig. 8. The simulation conditions are as follows: Irradiance D 1000 W/m2, Temperature D 25◦C), the load power PL D 8 kW. The DC bus voltage Vbus is controlled at the present value Vbus∗ D 500 V as shown in Fig. 8 (a). From Fig. 8 (b), Fig. 8 (c) and Fig. 8 (d), the MPPT loop is also enabled in this scenario and the PV operates at the maximum power point with VPV controlled near the ideal value VMPP D 435 V and IPV controlled near the ideal

International Journal For Advanced Research In Science & Technology
A peer reviewed international journal
www.ijarst.in
ISSN: 2457-0362

value IMPP D 22 A. According to Fig. 8 (e), the battery operates in the charging mode in this scenario and the surplus power from the PV can be stored in the battery.

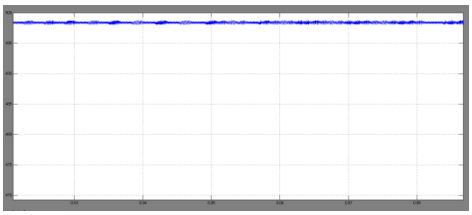

(a)

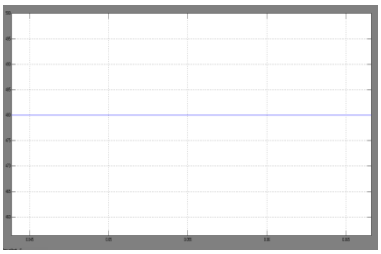

(b)

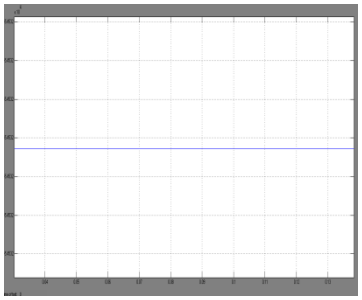

(c)

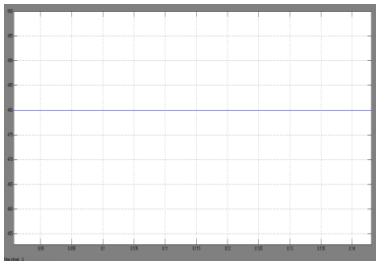

(d)

FIGURE 9 Steady state simulation results of operation scenario 5. (a) DC bus voltage Vbus; (b) PV voltage VPV; (c) PV current IPV; (d) Battery charging current ib

The steady state simulation results of the operation scenario 5 are shown in Fig. 9. The simulation conditions are as follows: Irradiance D 1000 W/m2, Temperature D 25 ◦C, the load power PL D 2:5 kW. The DC bus voltage Vbus is controlled at the preset value Vbus∗ D 500 V as shown in Fig. 10 (a). In this scenario the maximum charging current loop is enabled and the MPPT loop is disabled, and the battery charging current is controlled as i∗ b D 30 A, which is shown in Fig. 9 (d). From Fig. 9 (b) and Fig. 9 (c), the PV would not operate at the maximum power point in this scenario, in order to achieve the power balance of the system.

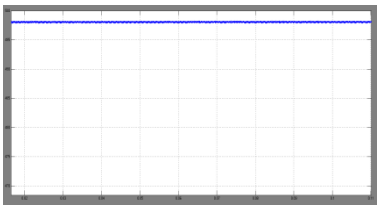

(a)

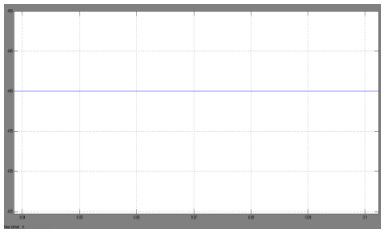

(b)

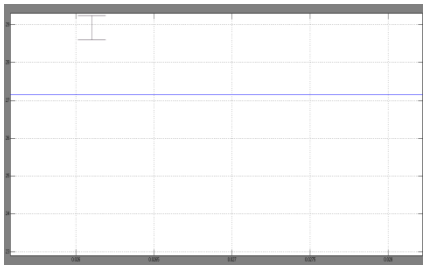

(c)

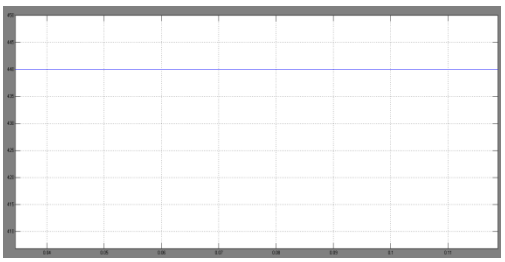

International Journal For Advanced Research In Science & Technology
A peer reviewed international journal
www.ijarst.in
ISSN: 2457-0362

(d)

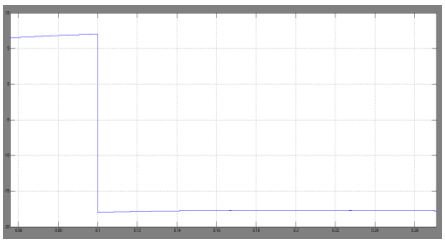

(e)

FIGURE 10. Simulation results with irradiance dropping from 1000 W/m2 to 500 W/m2 at t D 2 s. (a) DC bus voltage Vbus; (b) PV voltage VPV; (c) PV current IPV; (d) PV reference voltage Vref; (e) Battery charging current ib.

The dynamic performance of the system with the irradiance dropping from 1000 W/m2 to 500 W/m2 at t D 2 s is presented in Fig. 10. Other simulation conditions are as follows: Temperature D 25◦C, the load power PL D 8 kW. The DC bus voltage Vbus keeps stable during the transition as shown in Fig. 10 (a). In this scenario the MPPT loop always takes charge of the control of the duty cycle D. From Fig. 10 (d), there is a slight rise of the PV reference voltage Vref, due to the variation of the PV characteristic curve during the transition. From Fig. 10 (b) and Fig. 10 (c), MPPT is achieved with the PV operating near the maximum power points of the two characteristic curves. From Fig. 10 (e), the irradiance dropping incident can be considered as a transition from the scenario 4 to the scenario 2, as the battery operates in the charging mode before the transition and operates in the discharging mode after the transition.

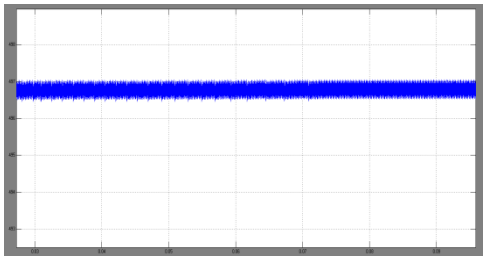

(a)

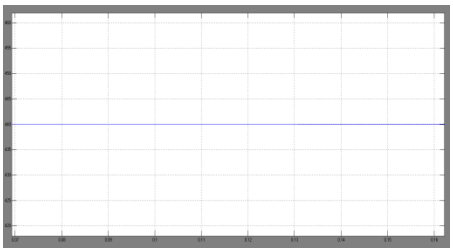

(b)

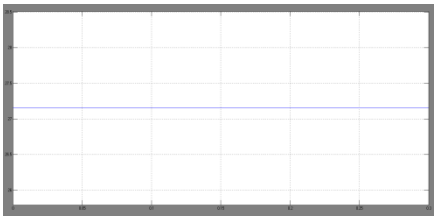

(c)

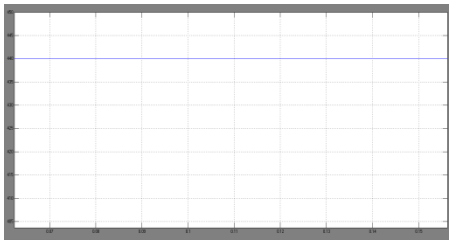

(d)

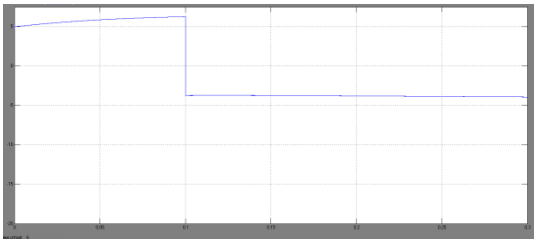

(e)

FIGURE 11. Simulation results with load power rising from 8 kW to 10 kW at t D 2 s. (a) DC bus voltage Vbus; (b) PV voltage VPV; (c) PV current IPV; (d) PV reference voltage Vref; (e) Battery charging current ib.

The dynamic performance of the system with the load power PL rising from 8 kW to 10 kW at t D 2 s is presented in Fig. 11. Other simulation conditions are as follows: Irradiance D 1000 W/m2, Temperature D 25◦C. The DC bus voltage Vbus keeps stable during the transition as shown in Fig.

International Journal For Advanced Research In Science & Technology
A peer reviewed international journal
www.ijarst.in
ISSN: 2457-0362

11(a). In this scenario the MPPT loop is always enabled as shown from Fig. 11(b) to Fig. 11(d). Similar with the irradiance dropping incident discussed above, the load power rising incident can be considered as a transition from the operation scenario 4 to the scenario 2 as shown in Fig. 11(e).

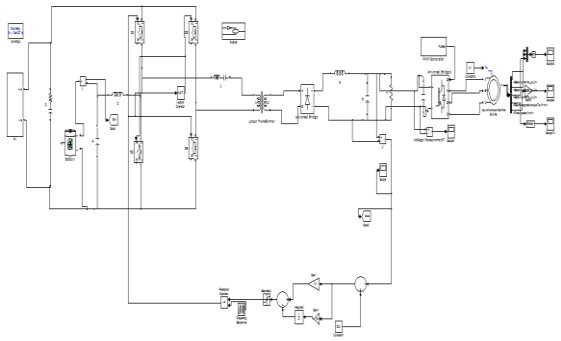

Fig 12 Simulink diagram of Proposed System power converter with Induction Motor drive

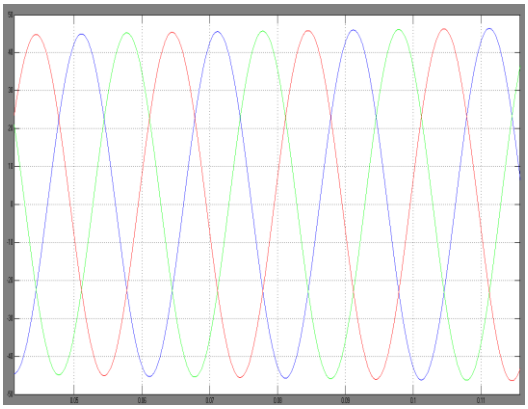

Fig 13 Simulation waveforms of Induction motor drive stator current characteristics

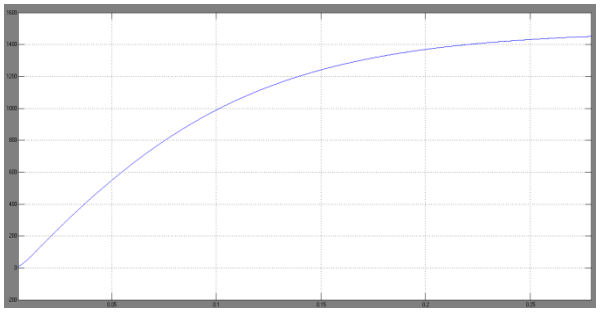

Fig 14 Simulation waveforms of Induction motor drive speed characteristics

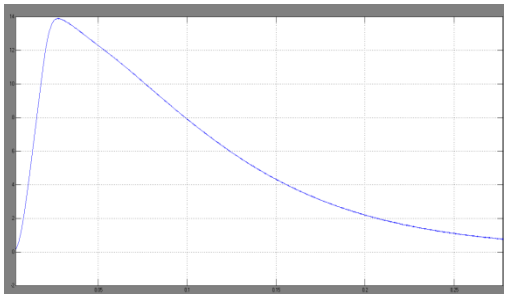

Fig 15 Simulation waveforms of Induction motor drive Torque characteristics

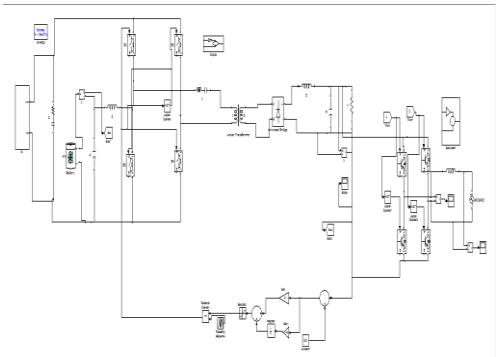

Fig 16 Simulink diagram of Proposed System power converter with Grid connected Systems

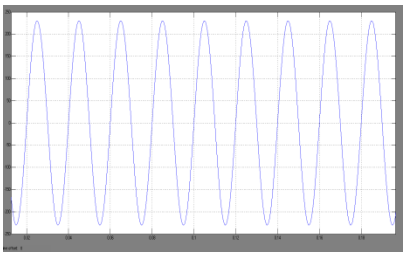

Fig 17 Simulation waveforms of Grid connected proposed system characteristics

(6) CONCLUSION

An integrated three-port power converter with Induction motor drive and grid applications as the interface for the PV/battery hybrid distributed power generation system is proposed Induction motor drive and grid applications. Compared with the conventional system topology containing an independent DC-DC unidirectional conversion stage and a bidirectional conversion stage, the proposed system Induction motor drive and grid applications has advantages in terms of higher power density and reliability. The phase shift angle of the full bridge and the switch duty cycle are adopted as two control variables to obtain the required DC bus voltage and realize

the power balance among three ports. Different operating scenarios of the system under various power conditions are discussed in detail and a comprehensive energy management and control strategy is proposed accordingly. The priority controller can enable one of the control loops in different scenarios to optimize the whole system performance, taking both the MPPT benefit and the battery charging/discharging management requirements into consideration. The simulation results verify the performance of the proposed Induction motor drive and grid applications PV/battery hybrid distributed power generation system and the feasibility of the control algorithm.

REFERENCES

[1] F. Blaabjerg, Z. Chen, and S. B. Kjaer, ‘‘Power electronics as efficient interface in dispersed power generation systems,’’ IEEE Trans. Power Electron., vol. 19, no. 5, pp. 1184–1194, Sep. 2004.

[2] J. M. Carrasco, L. G. Franquelo, J. T. Bialasiewicz, E. Galvan, R. Potillo, M. M. Prats, J. I. Leon, and N. Moreno-Alfonso, ‘‘Power-electronic systems for the grid integration of renewable energy sources: A survey,’’ IEEE Trans. Ind. Electron., vol. 53, no. 4, pp. 1002–1016, Jun. 2006.

[3] BP Statistical Review of World Energy, British Petroleum, London, U.K., Jun. 2018.

[4] J. P. Barton and D. G. Infield, ‘‘Energy storage and its use with intermittent renewable energy,’’ IEEE Trans. Energy Convers., vol. 19, no. 2, pp. 441–448, Jun. 2004.

[5] M. S. Whittingham, ‘‘History, evolution, and future status of energy storage,’’ Proc. IEEE, vol. 100, pp. 1518–1534, May 2012.

[6] C. A. Hill, M. C. Such, D. Chen, J. Gonzalez, and W. M. Grady, ‘‘Battery energy storage for enabling integration of distributed solar power generation,’’ IEEE Trans. Smart Grid, vol. 3, no. 2, pp. 850–857, Jun. 2012.

[7] Z. Yi, W. Dong, and A. H. Etemadi, ‘‘A unified control and power management scheme for PV-battery-based hybrid microgrids for both gridconnected and islanded modes,’’ IEEE Trans. Smart Grid, vol. 9, no. 6, pp. 5975–5985, Nov. 2018.

[8] H. Mahmood, D. Michaelson, and J. Jiang, ‘‘Decentralized power management of a PV/battery hybrid unit in a droop-controlled islanded microgrid,’’ IEEE Trans. Power Electron., vol. 30, no. 12, pp. 7215–7229, Dec. 2015.

[9] K. Sun, L. Zhang, Y. Xing, and J. M. Guerrero, ‘‘A distributed control strategy based on DC bus signaling for modular photovoltaic generation systems with battery energy storage,’’ IEEE Trans. Power Electron., vol. 26, no. 10, pp. 3032–3045, Oct. 2011.

[10] S. Adhikari and F. Li, ‘‘Coordinated V-f and P-Q control of solar photovoltaic generators with MPPT and battery storage in microgrids,’’ IEEE Trans. Smart Grid, vol. 5, no. 3, pp. 1270–1281, May 2014.

[11] S. K. Kollimalla, M. K. Mishra, and N. L. Narasamma, ‘‘Design and analysis of novel control strategy for battery and supercapacitor storage system,’’ IEEE Trans. Sustain. Energy, vol. 5, no. 4, pp. 1137–1144, Oct. 2014.

[12] S. Wen, S. Wang, G. Liu, and R. Liu, ‘‘Energy management and coordinated control strategy of PV/HESS AC microgrid during Islanded operation,’’ IEEE Access, vol. 7, pp. 4432–4441, 2019.

[13] W. Jiang and B. Fahimi, ‘‘Multiport power electronic interface—Concept, modeling, and design,’’ IEEE Trans. Power Electron., vol. 26, no. 7, pp. 1890–1900, Jul. 2011.

[14] H. Krishnaswami and N. Mohan, ‘‘Three-port series-resonant DC–DC converter to interface renewable energy sources with bidirectional load and energy storage ports,’’ IEEE Trans. Power Electron., vol. 24, no. 10, pp. 2289–2297, Oct. 2009.

[15] H. Tao, J. L. Duarte, and M. A. M. Hendrix, ‘‘Three-port triple-half-bridge bidirectional converter with zero-voltage switching,’’ IEEE Trans. Power Electron., vol. 23, no. 2, pp. 782–792, Mar. 2008.

[16] Z. Qian, O. Abdel-Rahman, and I. Batarseh, ‘‘An integrated four-port DC/DC converter for renewable energy applications,’’ IEEE Trans. Power Electron., vol. 25, no. 7, pp. 1877–1887, Jul. 2010.

[17] H. Al-Atrash and I. Batarseh, ‘‘Boost-integrated phase-shift full-bridge converter for three-port interface,’’ in Proc. IEEE Power Electron. Spec. Conf., Jun. 2007, pp. 2313–2321.

[18] W. Li, J. Xiao, Y. Zhao, and X. He, ‘‘PWM plus phase angle shift (PPAS) control scheme for combined multiport DC/DC converters,’’ IEEE Trans. Power Electron., vol. 27, no. 3, pp. 1479–1489, Mar. 2012.

[19] T. Esram and P. L. Chapman, ‘‘Comparison of photovoltaic array maximum power point tracking techniques,’’ IEEE Trans. Energy Convers., vol. 22, no. 2, pp. 439–449, Jun. 2007.